Short communication

Stable BaCe$_{0.5}$Zr$_{0.3}$Y$_{0.16}$Zn$_{0.04}$O$_{3-\delta}$ thin membrane prepared by in situ tape casting for proton-conducting solid oxide fuel cells

Shangquan Zhang [a], Lei Bi [a], Lei Zhang [b], Zetian Tao [a], Wenping Sun [a], Haiqian Wang [b], Wei Liu [a,*]

[a] Department of Material Science and Engineering, University of Science and Technology of China, Hefei, Anhui 230026, PR China
[b] Hefei National Laboratory for Physical Sciences at Microscale, University of Science and Technology of China, Hefei, Anhui 230026, PR China

ARTICLE INFO

ABSTRACT

Stable BaCe$_{0.5}$Zr$_{0.3}$Y$_{0.16}$Zn$_{0.04}$O$_{3-\delta}$ (BCZYZ) thin membrane was successfully prepared by in situ tape casting/co-firing method for proton-conducting solid oxide fuel cells. The starting powders were BaCO$_3$, CeO$_2$, ZrO$_2$, Y$_2$O$_3$, ZnO for electrolyte and BaCO$_3$, CeO$_2$, ZrO$_2$, Y$_2$O$_3$, ZnO, NiO, graphite for anode. The anode/electrolyte bi-layers were prepared by a simple multi-layer tape casting/co-firing method. The phase characterizations and microstructures were studied by X-ray diffraction (XRD) and scanning electron microscopy (SEM). The anode–electrolyte bi-layers were sintered at 1450 °C. The electrolytes were extremely dense with pure perovskite phase and the thickness was about 25 μm. The anodes were porous and no obvious reaction was found between NiO and BCZYZ. With LaSr$_3$Co$_{1.5}$Fe$_{1.5}$O$_{10-\delta}$ (LSCF)/BCZYZ as cathode, the open current voltage and maximum power density respectively, reached 1.00 V and 247 mW cm^{-2} at 650 °C.

© 2008 Elsevier B.V. All rights reserved.

1. Introduction

Protonic ceramic conductors have become the promising candidate for intermediate temperature solid oxide fuel cells (ITSOFC) since Iwahara et al. found that some perovskite oxides showed excellent protonic conductivity at intermediate temperature [1]. The most prevailing protonic conductors were doped barium cerate and barium zirconia [2–4]. Barium cerate exhibits high protonic conductivity and poor stability, and barium zirconia shows high stability and poor conductivity [5,6]. It is found that barium cerate, when partial replaced at a desired fraction of Ce by Zr, exhibits adequate proton conductivity as well as sufficient chemical and thermal stability in CO$_2$ and steam conditions [7,8]. Fabrication of dense zirconate always needs high sintering temperature [9]. Babilo and Haile [10] and Tao and Irvine [11] solved these problems by introducing Zn into Y- and Zr-doped BaCeO$_3$, which not only lowered the sintering temperature, but also increased the stability of BaCeO$_3$-based materials. In Ref. [11], BaCe$_{0.5}$Zr$_{0.3}$Y$_{0.16}$Zn$_{0.04}$O$_{3-\delta}$ (BCZYZ) was considered as the optimized composition.

Tape casting/co-firing method is widely used in preparing oxygen ionic conducting electrolyte because of its potentially cost efficiency for mass production [12–14]. However, to the best of our knowledge, preparation of proton-conducting thin membrane by tape casting has not been reported to date. Difficulty in mass production of oxide proton conductor powders and their poor sinterability embarrassed the usage of this method in proton-conducting solid oxide fuel cells.

In our previous work, an extremely dense BaCe$_{0.8}$Sm$_{0.2}$O$_{3-\delta}$ thin membrane was successfully prepared by an in situ reaction method [15]. In this work, BCZYZ electrolyte and BCZYZ/NiO anode were prepared by a novel method of multi-layer tape casting/co-firing method based on in situ reaction method. The effect of sintering temperature on the morphology of BCZYZ electrolyte and the performance of single cell were also studied.

2. Experimental

The anode–electrolyte bi-layers were prepared by in situ tape casting/co-firing method. The composition of anode substrate and electrolyte slurry was shown in Table 1. The starting powders were BaCO$_3$, CeO$_2$, ZrO$_2$, Y$_2$O$_3$, ZnO for electrolyte and BaCO$_3$, CeO$_2$, ZrO$_2$, Y$_2$O$_3$, ZnO, NiO, graphite for anode. The slurries for tape casting were prepared by a two-step ball milling process. In the first step, all the metal oxide and metal carbonate powder were homogeneously dispersed in ethanol/2-butanone solvent, with triethanolamine as the dispersant. Secondly, polyvinyl butyral (PVB), polyethylene glycol (PEG) and dibutyl *o*-phthalate (DBP) were added as binders and plasticizers to provide appropriate viscosity of the slurry.

The tape casting procedure also included two steps. Firstly, the de-aired electrolyte slurry was casted on the Mylar membrane at the blade height of about 0.05 mm. Secondly, the de-aired anode slurry was casted on the dried electrolyte tape, which should be

Table 1
Composition of the tape casting slurry.

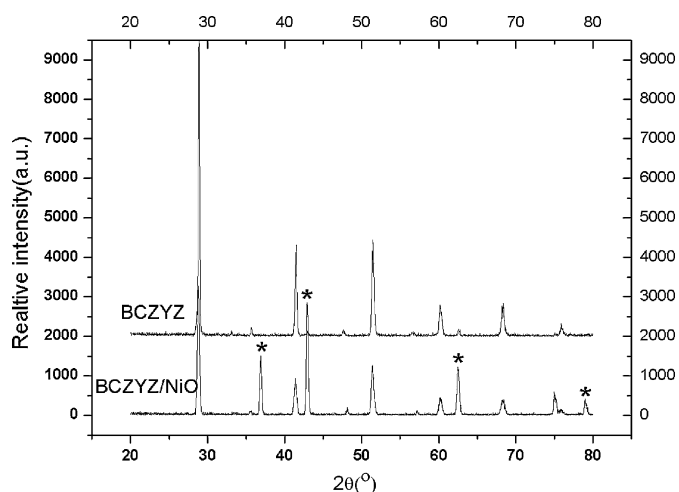|	Powder	Pore former	Solvent	Dispersant	Binder	Plasticizer
Anode	$BaCO_3$, CeO_2, Y_2O_3, ZrO_2, ZnO, NiO	Graphite	Ethanol/2-butanone	Triethanolamine	PVB	PEG/DBP
Electrolyte	$BaCO_3$, CeO_2, Y_2O_3, ZrO_2, ZnO	None	Ethanol/2-butanone	Triethanolamine	PVB	PEG/DBP

Fig. 1. XRD spectra of (a) BCZYZ electrolyte and (b) BCZYZ/NiO, *NiO.

carefully protected from being destroyed, at the blade height of about 2.5 mm. After dried for 24 h, the bi-layer green tapes were cut into 40 mm × 40 mm rectangular sheet and co-fired at different temperatures.

The cathode slurry, which was prepared by mixing LSCF and BCZYZ powders, synthesized by GNP method, and ethyl cellulose and terpineol (0.5:0.5:1 at weight ratio), was screen-printed on the electrolyte and fired at 1000 °C for 3 h. The active area of cathode was about 2 cm²; silver paste was applied as cathode current collector. Humidified hydrogen (3% H_2O) was fed to the anode chamber at a flow rate of 92 ml min⁻¹, while the cathode was exposed to atmospheric air. The anode side was sealed with Ag paste on the stainless steel box which acted as anode chamber.

Fuel cell performance was measured with DC Electronic Load (IT8511). Resistances of the cell under open circuit condition were measured at between 550 °C and 700 °C by CHI604B (0.1 Hz to 100 kHz). The phase characterizations were examined with X-ray diffractometer (XRD) using Cu Kα radiation by testing the surface
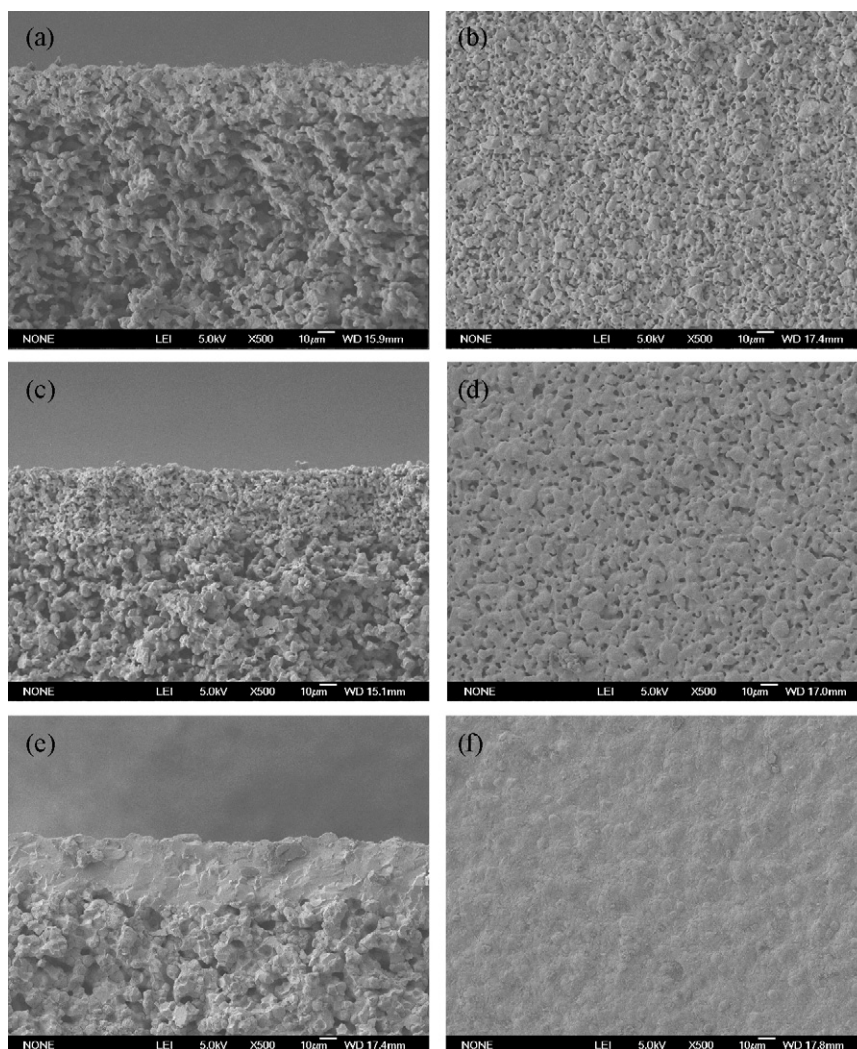

Fig. 2. The microstructure of electrolyte and anode which were sintering at different temperatures:fracture morpology of (a) 1350 °C, (c) 1400 °C, and (e) 1450 °C and surface morpology (b) 1350 °C, (d) 1400 °C, and (f) 1450 °C.

of the sintered electrolyte membrane and anode substrate. The fracture and surface morphology of the electrolyte and single cell were tested by scanning electron microscope (SEM, JSM-6301F).

The conductivity of pure BCZYZ was measured on CHI604B (0.1 Hz to 100 kHz) in a wet hydrogen (~3%) atmosphere. The sample pellets were prepared by dry-pressing BCZYZ powder and sintering at 1450 °C, Ag paste was printed on the both sides of the sample pellets. The Evolve Circuit software was used to analyze the impedance data and to calculate the conductivity of the samples.

3. Results and discussion

3.1. Phase characterization of BCZYZ

Fig. 1 showed the XRD spectra of the BCZYZ electrolyte (Fig. 1a) and BCZYZ/NiO anode (Fig. 1b) after sintering at 1450 °C. As can be seen in Fig. 1a, XRD peaks were identical with those of the barium cerate standard (JCPDS Card No. 82-2425), which were also identical with those of the BCZYZ in literatures [11,16]. Fig. 1b presented the XRD pattern of BCZYZ/NiO anodes. The peak lines of BCZYZ and NiO were separated well. The XRD data suggested that there were no observable chemical reactions between NiO and BCZYZ in the anodes which were prepared by in situ tape casting/co-sintering.

3.2. Microstructure of electrolyte and anode

Fig. 2 showed the fracture and surface morphology of the BCZYZ electrolyte after sintered at different temperatures. As can be seen, the electrolytes were porous after sintered at 1350 °C and 1400 °C but fully dense after sintered at 1450 °C. The porosity of the anode also decreased as the sintering temperature increased.

Tao and Irvine [11] reported that the sintering temperature of bulk $BaCe_{0.5}Zr_{0.3}Y_{0.16}Zn_{0.04}O_{3-\delta}$ can be decreased to 1325 °C by adding Zinc which was an effective sintering aid. BCZYZ/BCZYZ–NiO bi-layers were prepared by dry-pressing and co-firing at 1250 °C at Ref. [16]. The sintering temperature in our work was higher than those reported in Refs. [11,16], which may be attributed to the different process techniques. The green density of BCZYZ pellets which was prepared by dry-pressing was higher than that of those prepared by tape casting in our work. The green tapes had 20 wt.% organic additives, which decreased the green density and increased the difficulty of sintering.

The in situ tape casting/co-sintering method had the advantages of combining phase formation and forming process at a single sintering step [15]. The phase formation temperature of doped barium cerate which was prepared by solid-state reaction was about 1200 °C and the sintering temperature was about 1500 °C [17,18]. In our work, after sintering at 1450 °C, the BCZYZ electrolyte was pure phase and fully dense.

3.3. Performance of single cells

Fig. 3 showed the SEM photos of cross-section morphology of the single cell after testing. It can be seen that the BCZYZ electrolyte was very dense with the thickness of about 25 μm. No delaminations and cracks were found at the interface of electrode and electrolyte. Fig. 4 showed the performance of a single cell. The open circuit voltage was 1.03 V, 1.02 V, 1.00 V, and 0.95 V at 550 °C, 600 °C, 650 °C, and 700 °C, respectively which was close to the theoretical values 1.159 V, 1.152 V, 1.147 V, 1.141 V at 550 °C, 600 °C, 650 °C, and 700 °C which were calculated by Nernst equation, indicating that the electrolyte membrane was gas tight. The maximal power density was 56 mW cm^{-2} at 550 °C, 175 mW cm^{-2} at 600 °C, 250 mW cm^{-2} at 650 °C, and 275 mW cm^{-2} at 700 °C. Fig. 5 showed the result of impedance spectroscopy measured under open circuit condition. The total ohmic resistance of the cell, including ionic resistance of
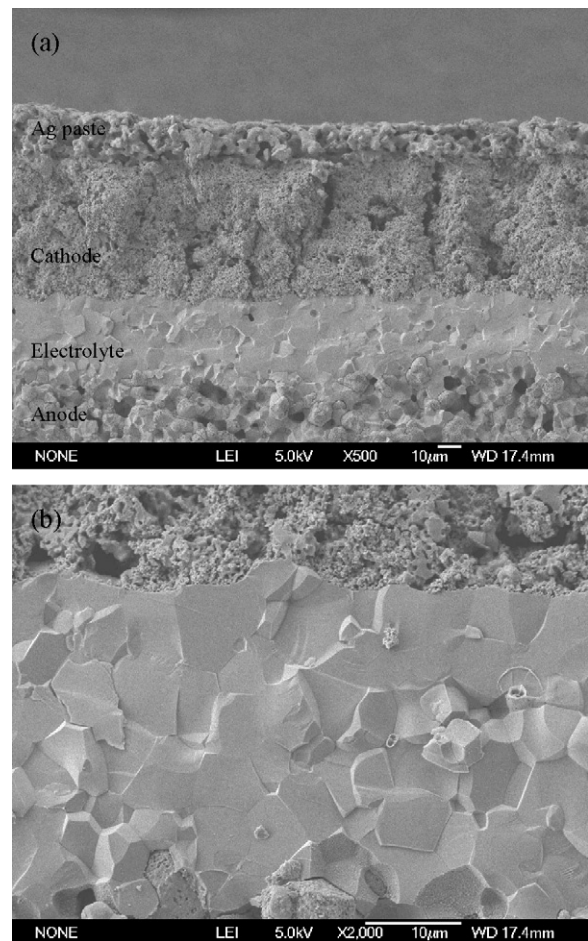

Fig. 3. Microstructure of single cell (a) cross-section of single cell and (b) larger magnification of interface between electrolyte and cathode.

the electrolyte, electronic resistance of the electrodes and some contact resistance associated with interfaces is corresponded to the high frequency intercept [19]. The ohmic resistance of the cell is usually taken as the overall electrolyte resistance of the cell (or area specific resistance, Ra) as the electronic resistance of the electrodes is small and can be ignored [20]. The low frequency intercept corresponds to the polarization resistance of the cell. Therefore,
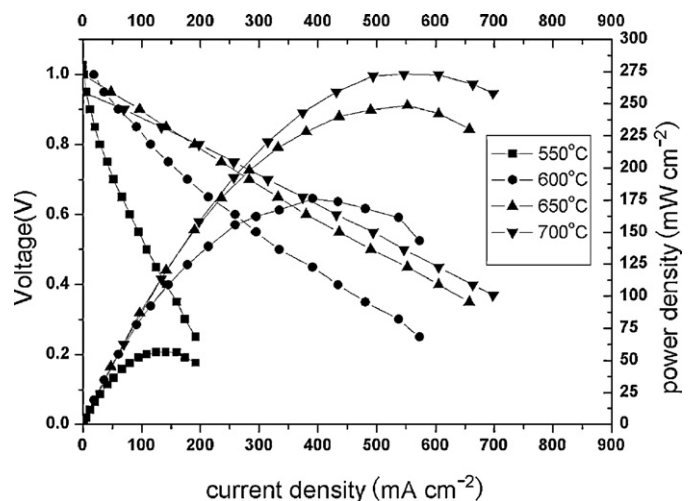

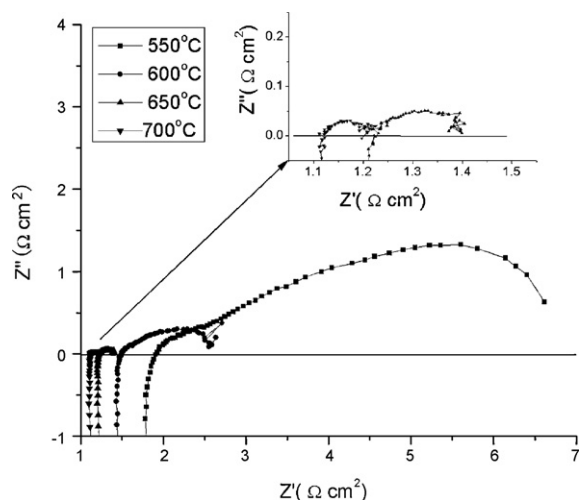**Fig. 4.** Performance of a single cell with humidified hydrogen measured at 550 °C, 600 °C, 650 °C and 700 °C.

Fig. 5. Impedance spectra of the single cell measured at 550 °C, 600 °C, 650 °C and 700 °C under open circuit condition.
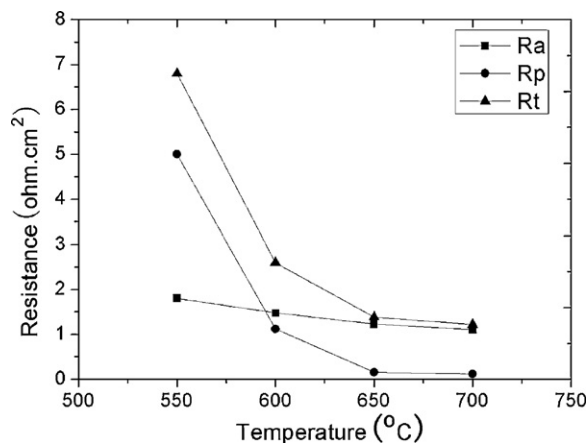

Fig. 6. The area specific resistance (Ra), polarization resistance (Rp), and total resistances (Rt) determined from the impedance spectra of the as-prepared cell measured under open-circuit conditions at 550 °C, 600 °C, 650 °C and 700 °C.
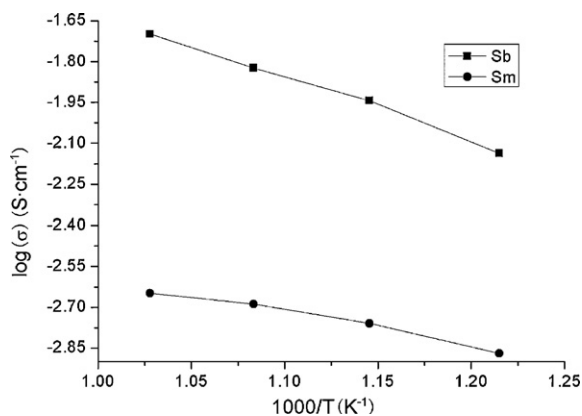

Fig. 7. Conductivities of pure BCZYZ pellet (Sb) and BCZYZ membrane (Sm) determined from Ra at 550 °C, 600 °C, 650 °C and 700 °C.

the total interfacial polarization resistance (Rp) of the cell can be obtained by subtracting the high frequency intercept from the low frequency intercept. Thus, it can be seen from Fig. 6 that the Ra of the cell was $1.85\,\Omega\,cm^2$, $1.44\,\Omega\,cm^2$, $1.23\,\Omega\,cm^2$, and $1.11\,\Omega\,cm^2$

at 550 °C, 600 °C, 650 °C, and 700 °C, respectively. Assuming the cell resistance mostly came from the electrolyte, the conductivity of BCZYZ (25 μm) were $2.25 \times 10^{-3}\,S\,cm^{-1}$, $2.03 \times 10^{-3}\,S\,cm^{-1}$, $1.74 \times 10^{-3}\,S\,cm^{-1}$, and $1.35 \times 10^{-3}\,S\,cm^{-1}$ at 700 °C, 650 °C, 600 °C, and 550 °C, respectively. The values were quite close to the article mentioned above [16]. The conductivity of BCZYZ membrane was six times smaller than bulk conductivity of pure BCZYZ (Fig. 7), which may be attributed to constriction of current pathways and the microstructure at the electrode/electrolyte interface [21]. The values of polarization resistance (Rp) were $5.06\,\Omega\,cm^2$, $1.12\,\Omega\,cm^2$, $0.16\,\Omega\,cm^2$, and $0.12\,\Omega\,cm^2$ at 550 °C, 600 °C, 650 °C, and 700 °C, respectively. The sharp increasing of Rp at 550 °C indicated that the performance of LSCF cathode was very poor on the proton-conducting electrolyte when the operating temperature was lower than 600 °C.

4. Conclusions

Dense protonic electrolyte membrane and porous anode substrate of $BaCe_{0.5}Zr_{0.3}Y_{0.16}Zn_{0.04}O_{3-\delta}$ (BCZYZ)/BCZYZ–NiO were prepared by a simple and effective method of in situ tape casting/co-sintering, the thickness of BCZYZ electrolyte was about 25 μm. With LSCF as cathode, single cell was assembled and tested at different temperature. The open circuit voltage and maximum power density of the cell were 1.03 V, 1.02 V, 1.00 V, 0.95 V and $56\,mW\,cm^{-2}$, $175\,mW\,cm^{-2}$, $250\,mW\,cm^{-2}$, and $275\,mW\,cm^{-2}$ at 550 °C, 600 °C, 650 °C, 700 °C, respectively. To sum up, this novel method can be considered as a quite promising membrane fabrication technique for the future commercialization of proton-conducting solid oxide fuel cells.

Acknowledgements

References

[1] H. Iwahara, H. Uchida, K. Ono, K. Ogaki, J. Electrochem. Soc. 135 (1988) 529–533.
[2] J. Wu, S.M. Webb, S. Brennan, S.M. Haile, J. Appl. Phys. 97 (1) (2005) 054101.
[3] J.-X. Wang, W.-H. Sub, J. Alloys Compd. 421 (2006) 45–48.
[4] P. Ranran, W. Yan, Y. Lizhai, Solid State Ionics 177 (2006) 389–393.
[5] Rinlee Butch Cervera, Yukiko Oyama, Shogo Miyoshi, Kiyoshi Kobayashi, Takehiko Yagi, Shu Yamaguchi, Solid State Ionics 179 (2008) 236–242.
[6] N. Bonanos, K.S. Knight, B. Ellis, Solid State Ionics 79 (1995) 161–170.
[7] Chendong Zuo, Shaowu Zha, Meilin Liu, Masaharu Hatano, Makoto Uchiyama, Adv. Mater. 18 (2006) 3318–3320.
[8] K. Katahira, Y. Kohchi, T. Shimura, H. Iwahara, Solid State Ionics 138 (2000) 91–98.
[9] H.G. Bohn, T. Schober, J. Am. Ceram. Soc. 83 (2000) 768–772.
[10] P. Babilo, S.M. Haile, J. Am. Ceram. Soc. 88 (2005) 2362–2368.
[11] S.W. Tao, J.T.S. Irvine, Adv. Mater. 18 (2006) 1581–1584.
[12] D. Montinaro, V.M. Sglavo, Solid State Ionics 177 (2006) 2093–2097.
[13] Zhenrong Wang, Jiqin Qian, Jiadi Cao, Shaorong Wang, Tinglian Wen, J. Alloys Compd. 437 (2007) 264–268.
[14] Hwan Moon, Sun Dong Kim, Sang Hoon Hyun, Ho Sung Kim, Int. J. Hydrogen Energy 33 (2008) 1758–1768.
[15] Lei Bi, Shangquan Zhang, Electrochem. Commun. 10 (2008) 1005–1007.
[16] Bin Lin, Mingjun Hu, Jianjun Ma, Yinzhu Jiang, Shanwen Tao, Guangyao Meng, J. Power Sources 183 (2008) 479–484.
[17] M. Ahrens, J. Maier, Thermochim. Acta 443 (2006) 189–196.
[18] Shinsuke Yamanak, Tsuyoshi Hamaguchi, Taku Oyam, Tetsushi Matsud, Shinichi Kobayashi, Ken Kurosaki, J. Alloys Compd. 359 (2003) 1–4.
[19] K.J. Yoon, W.H. Huang, G.S. Ye, S. Gopalan, U.B. Pal, D.A. Seccombe, J. Electrochem. Soc. 154 (2007) B389.
[20] L. Zhang, S.P. Jiang, W. Wang, Y.J. Zhang, J. Power Sources 170 (2007) 55–60.
[21] P.K. Srivastava, T. Quach, Y.Y. Duan, R. Donelson, S.P. Jiang, F.T. Ciacchi, S.P.S. Badwal, Solid State Ionics 99 (1997) 311–319.